Int. J. Anal. Appl. (2024), 22:209

International Journal of Analysis and Applications

A New Operational Matrices Based-Technique for Fractional Integro Reaction-Diffusion Equation Involving Spatiotemporal Variable-Order Derivative

Moustafa Ahmed[1], Hoda F. Ahmed[2], W. A. Hashem[2,*]

[1]*Department of Physics, Faculty of Science, King Abdulaziz University, 80203, Jeddah, 21589, Saudi Arabia*

[2]*Mathematics Department, Faculty of Science, Minia University, Minia, Egypt*

[*]*Corresponding author:* waleed.hashim@mu.edu.eg

Abstract. In this article, a novel generalized model of the nonlinear fractional integro-reaction-diffusion equation (NFIRDE) with spatiotemporal variable-order (SVO) is introduced, where the variable order derivatives are equipped with the Atangana–Baleanu–Caputo (ABC) sense. This model represents a great generalization of a significant type of NFIRDE and their applications. Moreover, A novel, efficient and fully spectral shifted Legendre tau technique is developed to solve the proposed model. Despite the difficulty of applying this mechanism to solve this type of equations, due to the presence of nonlinear terms and the SVO functions that appear in the traditional differential and integral operational matrices. We deduce some new operational matrices that play the fundamental role in facilitating the implementation of the tau method. These operational matrices represent the SVO ABC-derivative, the integro term within the model, as well as the vector multiplications with the space-time Kronecker product. As a result, the proposed model is restructured into a system of nonlinear algebraic equations, which simplifying the solving process. We illustrate our method's effectiveness and validity with numerical examples with both smooth and non-smooth solutions. Our findings show that the proposed tau method delivers accurate results and exhibits non-local properties.

1. Introduction

During the preceding thirty years, fractional calculus has become a focus of study due to its applications in a variety of scientific and engineering domains [1–3]. This concept has also been effectively employed to represent practical scenarios in various fields [4–7]. In variable-order fractional calculus, the focus is on differentiating and integrating with fractional orders that can vary in terms of known functions of independent variables [8–10]. This differs from standard fractional calculus, which maintains fixed constants for the orders of derivatives and integrals.

Received: Sep. 26, 2024.

2020 *Mathematics Subject Classification.* 65D32, 34K08, 35R11.

Key words and phrases. Atangana–Baleanu fractional derivative; spatiotemporal variable-order; nonlinear integro reaction-diffusion equation; shifted Legendre polynomials; spectral tau method.

https://doi.org/10.28924/2291-8639-22-2024-209
ISSN: 2291-8639

Practical systems modeled by these emerging interdisciplinary approaches in physics, finance, engineering and biology demonstrate improved sensitivity and precision when using variable-order fractional operators [11–13]. The variable-order fractional calculus can be perceived as pseudo-differential operators [14]. Additional characteristics of different kinds of variable-order fractional derivatives such as Grünwald-Letnikov, Riesz, Caputo, Riemann-Liouville, and ABC were explored in [15,16].

The ABC fractional derivative kernel is associated with the Mittag-Leffler function $E_\alpha(t)$ with a positive parameter α $\left(E_\alpha(t) = \sum_{r=0}^{\infty} \frac{t^r}{\Gamma(r\alpha+1)}\right)$ and generates derivatives according to the generalized Mittag-Leffler law $E_{\alpha,\beta}(t)$ $\left(E_{\alpha,\beta}(t) = \sum_{r=0}^{\infty} \frac{t^r}{\Gamma(r\alpha+\beta)}\right)$ while exhibiting Dirac-Delta properties [17]. In the chaotic problems, the ABC fractional derivative yields an infinite expectation value. Moreover, it serves as an effective modelling tool for dynamical systems occurring within the Penrose tiling space, notable for its non-periodic characteristics. This derivative also finds utility in describing fractal models within an undividable unitary space representations of discrete groups and foliation leaf spaces. In addition, the ABC fractional derivative proves valuable to address the Brillouin zone in studies pertaining to the quantum Hall effect and for characterizing State spaces in the realm of quantum mechanics. Its application is particularly advantageous in scenarios where the distribution of waiting times remains independent of elapsed time during specific events [18]. The asymptotic behaviour of the ABC derivative aligns with power law behaviour and establishes a connection between historical concepts of fading memory and non-singular kernels [19]. Additionally, the mean square displacement of the ABC fractional derivative exhibits a transition from conventional to sub-diffusive behaviour.

The nonlinear partial differential equations are investigated in pursuit of simulating diverse physical phenomena present in a wide range of scientific disciplines. These encompass areas like heat conduction in materials with memory, plasma physics and water wave dynamics, as documented in the reference [20]. However, in some applications, such as dynamics of nuclear reactors and thermoelastic phenomena, it becomes necessary to account for the inherent memory influence within systems. While utilizing partial differential equations to model these systems, which traditionally incorporate functions at specific temporal and spatial points, the historical aspect often gets disregarded. To address this memory effect, an integration term is introduced into the partial differential equation formulation. Partial integro-differential equations find extensive utility in chemical reaction kinetics, control theory, aerospace engineering, biological systems modeling and financial mathematics, as well as industrial mathematics [21].

The nonlinear reaction diffusion and integro reaction-diffusion equations are frequently applied to explain different types of phenomena such as the skin or fur of mammals [22], the physics of hot plasmas [23], Chemical oscillation waves and turbulence [5], spatial pattern formation in biological contexts [24] and the evolution of concentrations in environmental and biological applications [4]. In the mechanism of reaction-diffusion, the progression involves the movement of reacting molecules through space as a consequence of diffusion. This definition specifically omits

additional transport modes such as convection or drift, which might emerge in the presence of externally applied fields. Within a spatial unit where a reaction takes place, molecules can either be generated or depleted. These occurrences are incorporated into the diffusion equation, resulting in the formulation of a reaction-diffusion equation. Lately, the fractional representation of the reaction-diffusion equation and integro reaction-diffusion equations have attracted considerable attention from a wide range of aspects; for example, see [21, 25–31] and references therein.

In this paper, the focus is on the SVO ABC NFIRDE

$$ {}^{ABC}_{0}\mathcal{D}_{t}^{\xi(x,t)}\Phi(x,t) = a_1\,\Phi(x,t) - a_2\,\Phi^2(x,t) + a_3\left(\Phi(x,t)\right)^r \int_0^t k(x,s)\,\Phi(x,s)ds + a_4\,\frac{\partial^2\Phi(x,t)}{\partial x^2} + f(x,t), \tag{1.1} $$

along the initial and boundary conditions (IBCs):

$$ \begin{aligned} &\Phi(x,0) = g(x), \\ &\Phi(0,t) = h_1(t), \quad \Phi(l,t) = h_2(t). \end{aligned} \tag{1.2} $$

Here, $(x,t) \in [0,l]\times[0,T]$, $0 < \xi(x,t) \le 1$, $a_1 \ge 0, a_2 \ge 0, a_3 \ge 0, a_4 > 0, r = \{0,1\}$ and ${}^{ABC}_{0}\mathcal{D}_{t}^{\xi(x,t)}\Phi(x,t)$ is the ABC time fractional differential operator with SVO which is defined as

$$ {}^{ABC}_{0}\mathcal{D}_{t}^{\xi(x,t)}\Phi(x,t) = \frac{\mathcal{M}(\xi(x,t))}{1-\xi(x,t)} \int_0^t \frac{\partial\Phi(x,s)}{\partial s}\, E_{\xi(x,t)}\Big(\frac{-\xi(x,t)\,(t-s)^{\xi(x,t)}}{1-\xi(x,t)}\Big)ds, \tag{1.3} $$

where $\mathcal{M}(\xi(x,t)) = 1-\xi(x,t)+\frac{\xi(x,t)}{\Gamma\xi(x,t)}, \mathcal{M}(0) = \mathcal{M}(1) = 1$. Based on Eq. (1.3), the following relation for $n \in \mathbb{N}$ is satisfied [21]

$$ {}^{ABC}_{0}\mathcal{D}_{t}^{\xi(x,t)}t^n = \frac{\mathcal{M}(\xi(x,t))\;n!\;t^n}{1-\xi(x,t)}\, E_{\xi(x,t),n+1}\Big(\frac{-\xi(x,t)\;t^{\xi(x,t)}}{1-\xi(x,t)}\Big). \tag{1.4} $$

Note that, for $a_3 = 0$, Eq. (1.1) turns into the reaction-diffusion equation.

The systems that incorporate SVO fractional operators present a complicated challenge when searching for analytical solutions. Even when such solutions are successfully derived, they often involve many functions that pose significant computational difficulties. Hence, numerical methods are better suited for obtaining approximate solutions in such cases [32–34]. Currently, numerous researchers have proposed three main numerical techniques for effectively solving the variable order fractional differential equations: the spectral method, the finite element method and the finite difference method (see [30] and reference therein). There has been a growing interest in spectral methods for solving various types of differential, integral and integro-differential equations, primarily due to their flexibility in handling finite and infinite domains. Spectral methods represent the tau, collocation, Galerkin, and Petrov-Galerkin methods. These methods offer notable advantages, including exponential convergence rates and high accuracy.

As far as our knowledge extends, there are limited prior studies dedicated to the approximate solutions of the NFIRDE that incorporate the ABC variable-order fractional derivative. Kumar et al. [21] presented a discretization approach employing the quasi-wavelet method to discretize both

the spatial derivative and the unknown function. Furthermore, the ABC time fractional derivative was discretized with the help of Taylor series expansion for solving the constant-order ABC time fractional nonlinear reaction-diffusion equation and NFIRDE. Heydari et al. [35] introduced an operational matrix approach formulating a numerical method for the ABC variable-order fractional reaction-diffusion equation using shifted second kind Chebyshev cardinal functions. Kumar et al. [36] developed a numerical approach employing quasi-wavelets for solving reaction-diffusion and NFIRDE including constant order fractional derivatives, where the fractional component in the time dimension is approximated using the Crank-Nicolson scheme. Additionally, the spatial and integral components within the NFIRDE are discretized and approximated through the utilization of quasi-wavelets. Hosseininia et al. [27] introduced an effective semi-discrete approach utilizing two-dimensional Legendre wavelets. In this method, the variable order derivatives are estimated using a finite difference scheme, combined with the theta-weighted technique, to yield approximate solutions for the nonlinear two-dimensional reaction-diffusion equations involving ABC variable-order time fractional derivatives.

Accordingly, the main aim of this paper is to introduce a novel numerical approach for addressing the NFIRDE with ABC SVO time fractional derivative. This approach is based on a fully spectral shifted Legendre tau technique. It is known that applying this technique is very difficult, especially for this type of equations that contains the SVO derivative and non-linear terms. In order to solve these problems that obstruct the application of the technique used, a number of novel operational matrices have been derived, which include the operational matrix for the ABC time fractional derivatives of SVO, the integral term and vector multiplications with the space-time Kronecker product. These operational matrices enable us to apply a completely tau method effectively, even in the presence of nonlinear terms and the SVO functions that appeared within the SVO derivative operational matrix. As a result, equations (1.1) and (1.2) are restructured into a system of nonlinear algebraic equations, which simplifying the solving process. Our findings affirm that nonlocal numerical techniques are particularly well-suited for discretizing fractional integro-partial differential equations, as they inherently consider the global characteristics of the solution. It's worth emphasizing that substituting the variable order with a constant function leads to the conversion of variable order derivatives into fixed order derivatives. The authors believe that there is no previous work comprehensively utilizes the spectral tau technique for approximating solutions to the nonlinear integro-partial differential equations with ABC SVO time fractional derivative.

This paper is structured as follows: Section 2 provides a review of the mathematical foundations of Legendre polynomials. Section 3 presents the derivation of shifted Legendre operational matrices for SVO time fractional derivatives in the ABC sense, along with the multiplication and integration of space-time Kronecker product vectors. The detailed description of the proposed technique is given in Section 4. Section 5 contains various test examples to illustrate the method's applicability. Finally, Section 6 summarizes the findings of this paper.

2. Shifted Legendre polynomials and functions approximation

The Legendre polynomials $\mathcal{R}_j(t)$ of order j are orthogonal polynomials established over the interval $[-1,1]$ and is produced using the following Rodrigues' expression

$$\mathcal{R}_j(t) = \frac{(-1)^j}{2^j j!}\frac{d^j}{dt^j}\Big((t^2-1)^j\Big),$$

and satisfy the orthogonality relation

$$\langle \mathcal{R}_i(t), \mathcal{R}_j(t)\rangle = \int_{-1}^{1} \mathcal{R}_i(t)\mathcal{R}_j(t)dt = \frac{2}{2i+1}\delta_{i,j}. \tag{2.1}$$

To utilize these polynomials within the interval $t \in [0,T]$, we employ a variable transformation: $t \to \frac{2t}{T} - 1$. Let us represent the shifted Legendre polynomials by $\mathcal{R}_{T,j}(t) = \mathcal{R}_j(\frac{2t}{T} - 1)$, They fulfill the requirements of the following recurrence relation [37]:

$$\mathcal{R}_{T,0}(t) = 1,\ \mathcal{R}_{T,1}(t) = \frac{2t}{T} - 1,\ \mathcal{R}_{T,i+2}(t) = \frac{(2i+3)(2t-T)}{T(i+2)}\mathcal{R}_{T,i+1}(t) - \frac{i+1}{i+2}\mathcal{R}_{T,i}(t),\ i \geq 0.$$

Also, the following analytical formula is used to obtain the shifted Legendre polynomials

$$\mathcal{R}_{T,i}(t) = \sum_{k=0}^{i} \zeta_{ik}\, t^k, \qquad \zeta_{ik} = (-1)^{i+k}\frac{(k+i)!}{(i-k)!(k!)^2 T^k}, \tag{2.2}$$

with the following orthogonality relation

$$\langle \mathcal{R}_{T,i}(t), \mathcal{R}_{T,j}(t)\rangle = \int_0^T \mathcal{R}_{T,i}(t)\mathcal{R}_{T,j}(t)dt = \frac{T}{2i+1}\delta_{i,j} = J_T^{(i+1,j+1)}. \tag{2.3}$$

It is important to highlight that the sequence of shifted Legendre polynomials forms an L^2-orthogonal basis. Consequently, any function $\Phi(x,t) \in L^2([0,l]\times[0,T])$ can be represented using these basis functions in the following manner:

$$\Phi_{MN}(x,t) \simeq \sum_{i=0}^{M}\sum_{j=0}^{N} \psi_{ij}\, \mathcal{R}_{l,i}(x)\, \mathcal{R}_{T,j}(t) \simeq \Psi^\intercal \Big(\Theta_M(x)\otimes\Theta_N(t)\Big) \simeq \Big(\Theta_M(x)\otimes\Theta_N(t)\Big)^\intercal \Psi, \tag{2.4}$$

where $\otimes$ denotes the Kronecker product. Ψ and $\Big(\Theta_M(x)\otimes\Theta_N(t)\Big)$ are column vectors whose entries can be obtained as follows

$$\begin{aligned} \Psi =& [\psi_{00},...,\psi_{0N},\psi_{10},...,\psi_{1N},...,\psi_{M0},\psi_{M1},...,\psi_{MN}]^\intercal, \\ \psi_{ij} =& \frac{lT}{(2i+1)(2j+1)}\int_0^T\int_0^l \Phi(x,t)\, \mathcal{R}_{l,i}(x)\, \mathcal{R}_{T,j}(t)\, dxdt. \end{aligned} \tag{2.5}$$

$$\begin{aligned} &\Theta_M(x) = [\mathcal{R}_{l,0}(x), \mathcal{R}_{l,1}(x),..., \mathcal{R}_{l,M}(x)]^\intercal,\ \Theta_N(t) = [\mathcal{R}_{T,0}(t), \mathcal{R}_{T,1}(t),..., \mathcal{R}_{T,N}(t)]^\intercal, \\ &\Big(\Theta_M(x)\otimes\Theta_N(t)\Big) = [\mathcal{R}_{l,0}(x)\,\Theta_N(t), \mathcal{R}_{l,1}(x)\,\Theta_N(t),..., \mathcal{R}_{l,M}(x)\,\Theta_N(t)]^\intercal. \end{aligned} \tag{2.6}$$

Also, the Kronecker product satisfies the following important property for the matrices W, X, Y and Z

$$WX\otimes YZ = (W\otimes Y)(X\otimes Z). \tag{2.7}$$

Moreover, for simplicity in constructing the differentiation and integration operational matrices, the vector $\Theta_N(t)$ is rewritten in the following form

$$\Theta_N(t) = \theta_T \, \mathcal{B}_N(t), \tag{2.8}$$

where

$$\theta_T = \begin{pmatrix} \zeta_{0,0} & 0 & \dots & 0 \\ \zeta_{1,0} & \zeta_{1,1} & \dots & 0 \\ \vdots & \vdots & \ddots & \vdots \\ \zeta_{N,0} & \zeta_{N,1} & \dots & \zeta_{N,N} \end{pmatrix}, \; \mathcal{B}_N(t) = [1, t, t^2, ..., t^N]^\intercal. \tag{2.9}$$

3. Operational matrices

Herein, we establish the SVO ABC time fractional derivatives operational matrices, the vector multiplications with the space-time Kronecker product and the integration of the Kronecker product space-time vectors.

Theorem 3.1. *The ABC time-fractional derivative with SVO $\xi : [0, l][0, T] \to (0, 1)$ for the shifted Legendre vector $\Theta_N(t)$ can be formulated as*

$$ {}^{ABC}_{0}\mathcal{D}_t^{\xi(x,t)} \, \Theta_N(t) = \Upsilon^{\xi(x,t)} \, \Theta_N(t), \tag{3.1}$$

where

$$\Upsilon^{\xi(x,t)} = \frac{\mathcal{M}(\xi(x,t))}{1-\xi(x,t)} \sum_{k=1}^{N} k! \, E_{\xi(x,t),k+1}\Big(\frac{-\xi(x,t)\, t^{\xi(x,t)}}{1-\xi(x,t)}\Big) \, \theta_T \, \mathcal{T}_k \, \theta_T^{-1} \tag{3.2}$$

and $\mathcal{T}_k$ are $(N+1)\times(N+1)$ matrices defined by

$$\mathcal{T}_k = \Big[\tau_{ij}^k\Big]_{0\le i,j\le N}, \quad \tau_{ij}^k = \begin{cases} 1, & i = j = k, \\ 0, & \textit{otherwise}. \end{cases} \tag{3.3}$$

Proof. Taking into account the reformulating of the shifted Legendre vector $\Theta_N(t)$ in Eq. (2.8), we have

$$ {}^{ABC}_{0}\mathcal{D}_t^{\xi(x,t)} \, \Theta_N(t) = {}^{ABC}_{0}\mathcal{D}_t^{\xi(x,t)} \, \theta_T \, \mathcal{B}_N(t) = \theta_T \, {}^{ABC}_{0}\mathcal{D}_t^{\xi(x,t)} \, \mathcal{B}_N(t) \tag{3.4}$$

$$\begin{aligned} {}^{ABC}_{0}\mathcal{D}_t^{\xi(x,t)} \, \mathcal{B}_N(t) &= {}^{ABC}_{0}\mathcal{D}_t^{\xi(x,t)} \, [1, t, t^2, ..., t^N]^\intercal \\ &= \frac{\mathcal{M}(\xi(x,t))}{1-\xi(x,t)} \Big[0, 1! \, E_{\xi(x,t),2}\Big(\frac{-\xi(x,t)\, t^{\xi(x,t)}}{1-\xi(x,t)}\Big) t, 2! \, E_{\xi(x,t),3}\Big(\frac{-\xi(x,t)\, t^{\xi(x,t)}}{1-\xi(x,t)}\Big) t^2, \\ &\quad , ..., \, N! \, E_{\xi(x,t),N+1}\Big(\frac{-\xi(x,t)\, t^{\xi(x,t)}}{1-\xi(x,t)}\Big) t^N\Big]^\intercal \\ &= \frac{\mathcal{M}(\xi(x,t))}{1-\xi(x,t)} \Big(1! \, E_{\xi(x,t),2}\Big(\frac{-\xi(x,t)\, t^{\xi(x,t)}}{1-\xi(x,t)}\Big) \mathcal{T}_1 \, \mathcal{B}_N(t) + 2! \, E_{\xi(x,t),3}\Big(\frac{-\xi(x,t)\, t^{\xi(x,t)}}{1-\xi(x,t)}\Big) \mathcal{T}_2 \, \mathcal{B}_N(t) \end{aligned}$$

$$
\begin{aligned}
&+ \ldots + N!\, E_{\xi(x,t),N+1}\Big(\frac{-\xi(x,t)\, t^{\xi(x,t)}}{1-\xi(x,t)}\Big)\mathcal{T}_N\, \mathcal{B}_N(t)\Big) \\
&= \frac{\mathcal{M}(\xi(x,t))}{1-\xi(x,t)} \sum_{k=1}^{N} k!\, E_{\xi(x,t),k+1}\Big(\frac{-\xi(x,t)\, t^{\xi(x,t)}}{1-\xi(x,t)}\Big)\mathcal{T}_k\, \mathcal{B}_N(t).
\end{aligned} \tag{3.5}
$$

Now, by substituting from Eq. (3.5) in Eq. (3.4), we get

$$
{}^{ABC}_{0}\mathcal{D}_t^{\xi(x,t)}\, \Theta_N(t) = \frac{\mathcal{M}(\xi(x,t))}{1-\xi(x,t)} \sum_{k=1}^{N} k!\, E_{\xi(x,t),k+1}\Big(\frac{-\xi(x,t)\, t^{\xi(x,t)}}{1-\xi(x,t)}\Big)\theta_T\, \mathcal{T}_k\, \mathcal{B}_N(t). \tag{3.6}
$$

The invertibility of the matrix θ_T is established based on the orthogonality property of the shifted Legendre polynomials as described in Eq. (2.3). Consequently, the vector $\mathcal{B}_N(t)$ can be expressed in terms of $\Theta_N(t)$ as $\mathcal{B}_N(t) = \theta_T^{-1}\, \Theta_N(t)$, then Eq. (3.6) can be rewritten as follows

$$
{}^{ABC}_{0}\mathcal{D}_t^{\xi(x,t)}\, \Theta_N(t) = \Bigg(\frac{\mathcal{M}(\xi(x,t))}{1-\xi(x,t)} \sum_{k=1}^{N} k!\, E_{\xi(x,t),k+1}\Big(\frac{-\xi(x,t)\, t^{\xi(x,t)}}{1-\xi(x,t)}\Big)\theta_T\, \mathcal{T}_k\, \theta_T^{-1}\Bigg)\Theta_N(t), \tag{3.7}
$$

thus, the proof is completed.

Remark 1: Theorem 3.1 is a generalization of the shifted Legendre ABC fractional derivative with SVO. As a result, it can cover the constant order ABC fractional derivative by replacing the SVO $(\xi(x,t))$ by the constant order.

Theorem 3.2. *(See [38]) Let $\Theta_M(x)$ be the shifted Legendre vector, then the η integer-order derivative is obtained from*

$$
\frac{d^\eta}{dx^\eta}\, \Theta_M(x) = D^{(\eta)}\, \Theta_M(x), \tag{3.8}
$$

where $D^{(\eta)}$ represents an operational matrix of derivative with dimensionsis $(M+1)\times(M+1)$ and is defined by

$$
D^{(\eta)} = \Big[\varnothing_{ij}^{(\eta)}\Big]_{0\le i,j\le M},\ \varnothing_{ij}^{(\eta)} = \sum_{s=\eta}^{i}\sum_{r=0}^{s-\eta} \frac{(-1)^{i+r+s}\, (1+2r)\, ((i+s)!)\, (\eta-s)_r}{l^\eta\, ((i-s)!)\, (s!)\, \Gamma(2+r+s-\eta)}\delta_{i,j}. \tag{3.9}
$$

The following theorem will be crucial in completing the construction of the integral operational matrix. Additionally, it holds substantial importance in overcoming the challenges associated with the full implementation of the shifted Legendre tau method for Eq. (1.1) and Eq. (1.2). These challenges arise from the inclusion of known functions $\frac{\mathcal{M}(\xi(x,t))}{1-\xi(x,t)}\ \sum_{k=1}^{N} k!\, E_{\xi(x,t),k+1}\Big(\frac{-\xi(x,t)\, t^{\xi(x,t)}}{1-\xi(x,t)}\Big)$ in the SVO ABC time-fractional derivative operational matrix Eq. (3.1), as well as the presence of a nonlinear term within model Eq. (1.1).

Theorem 3.3. *Assume a continuously differentiable function $u(x,t)$ is approximated using shifted Legendre vectors as $u_{MN}(x,t) \simeq U^\intercal \Big(\Theta_M(x)\otimes\Theta_N(t)\Big)$ as stated in Eq. (2.4). Consequently, an $(M+1)\times(N+1)$ square matrix $\mathcal{U}$ exists and fulfills the following matrix approximation for the product of space-time*

Kronecker product vectors.

$$\Big(\Theta_M(x)\otimes\Theta_N(t)\Big)\Big(\Theta_M(x)\otimes\Theta_N(t)\Big)^{\intercal}U=\mathcal{U}^{\intercal}\Big(\Theta_M(x)\otimes\Theta_N(t)\Big), \tag{3.10}$$

where

$$\begin{aligned}\mathcal{U}&=[\mathcal{Z}_{0,0},...,\mathcal{Z}_{0,P},\mathcal{Z}_{1,0},...,\mathcal{Z}_{1,N},...,\mathcal{Z}_{M,0},\mathcal{Z}_{M,1},...,\mathcal{Z}_{M,N}],\\ \mathcal{Z}_{r,s}&=[C_{0,0,r,s},...,C_{0,N,r,s},C_{1,0,r,s},...,C_{1,N,r,s},...,C_{M,0,r,s},...,C_{M,N,r,s}]U,\end{aligned} \tag{3.11}$$

such that $\mathcal{Z}_{i,k}$ denotes the columns of matrix $\mathcal{U}$, where each element is acquired from

$$C_{i,j,r,s}=\frac{(2i+1)(2j+1)}{4}\left(\int_0^l\mathcal{R}_{l,p}(x)\mathcal{R}_{l,i}(x)\mathcal{R}_{l,r}(x)dx\right)\left(\int_0^T\mathcal{R}_{T,q}(t)\mathcal{R}_{T,j}(t)\mathcal{R}_{T,s}(t)dt\right). \tag{3.12}$$

Proof.: The left hand side of Eq. (3.10) can be written as

$$\Big(\Theta_M(x)\otimes\Theta_N(t)\Big)\Big(\Theta_M(x)\otimes\Theta_N(t)\Big)^{\intercal}U=\sum_{i=0}^{M}\sum_{j=0}^{N}u_{ij}\mathcal{R}_{l,i}(x)\mathcal{R}_{T,j}(t)\mathcal{R}_{l,r}(x)\mathcal{R}_{T,s}(t). \tag{3.13}$$

By approximating $\mathcal{R}_{l,i}(x)\mathcal{R}_{T,j}(t)\mathcal{R}_{l,r}(x)\mathcal{R}_{T,s}(t)$ for $r=0,1,\ldots,M$ and $s=0,1,\ldots,N$ as

$$\mathcal{R}_{l,i}(x)\mathcal{R}_{T,j}(t)\mathcal{R}_{l,r}(x)\mathcal{R}_{T,s}(t)=\sum_{p=0}^{M}\sum_{q=0}^{N}\chi_{p,q}^{i,j,r,s}\mathcal{R}_{l,p}(x)\mathcal{R}_{T,q}(t)=C_{i,j,r,s}\Big(\Theta_M(x)\otimes\Theta_N(t)\Big), \tag{3.14}$$

where $C_{i,j,r,s}=[\chi_{0,0}^{i,j,r,s},\chi_{0,1}^{i,j,r,s},...,\chi_{0,N}^{i,j,r,s},\chi_{1,0}^{i,j,r,s},\chi_{1,1}^{i,j,r,s},...,\chi_{1,N}^{i,j,r,s},...,\chi_{M,0}^{i,j,r,s},\chi_{M,1}^{i,j,r,s},...,\chi_{M,N}^{i,j,r,s}]^{\intercal}$ and

$$C_{i,j,r,s}=\frac{(2i+1)(2j+1)}{4}\left(\int_0^l\mathcal{R}_{l,p}(x)\mathcal{R}_{l,i}(x)\mathcal{R}_{l,r}(x)dx\right)\left(\int_0^T\mathcal{R}_{T,q}(t)\mathcal{R}_{T,j}(t)\mathcal{R}_{T,s}(t)dt\right).$$

From Eq. (3.13) and Eq. (3.14), we have

$$\begin{aligned}&\Big(\Theta_M(x)\otimes\Theta_N(t)\Big)\Big(\Theta_M(x)\otimes\Theta_N(t)\Big)^{\intercal}U=\sum_{i=0}^{M}\sum_{j=0}^{N}u_{ij}\sum_{p=0}^{M}\sum_{q=0}^{N}\chi_{p,q}^{i,j,r,s}\mathcal{R}_{l,p}(x)\mathcal{R}_{T,q}(t)\\ &=\sum_{p=0}^{M}\sum_{q=0}^{N}\mathcal{R}_{l,p}(x)\mathcal{R}_{T,q}(t)\sum_{i=0}^{M}\sum_{j=0}^{N}u_{i,j}\chi_{p,q}^{i,j,r,s}=\Big(\Theta_M(x)\otimes\Theta_N(t)\Big)^{\intercal}\mathcal{U}=\mathcal{U}^{\intercal}\Big(\Theta_M(x)\otimes\Theta_N(t)\Big),\end{aligned} \tag{3.15}$$

which completes the proof. □

Based on Theorem 3.3, suppose that the function $y(x,t)=t$ is approximated by using the shifted Legendre vectors as $y_{MN}(x,t)\simeq Y^{\intercal}\Big(\Theta_M(x)\otimes\Theta_N(t)\Big)=\Big(\Theta_M(x)\otimes\Theta_N(t)\Big)^{\intercal}\ Y$ as in Eq. (2.4). Then there is an $(M+1)\times(N+1)$ square matrix $\mathcal{Y}$ that satisfy the following relation

$$\Big(\Theta_M(x)\otimes\Theta_N(t)\Big)\Big(\Theta_M(x)\otimes\Theta_N(t)\Big)^{\intercal}Y=\mathcal{Y}^{\intercal}\Big(\Theta_M(x)\otimes\Theta_N(t)\Big). \tag{3.16}$$

In the following theorem, we introduce a shifted Legendre operational matrix for the integration of the vector formed by the Kronecker product across space and time.

Theorem 3.4. *The operational matrix of the integration of the vector formed by the Kronecker product across space and time is approximated as follows.*

$$\int_0^t \Big(\Theta_M(x) \otimes \Theta_N(s)\Big) ds = (I_{M+1} \otimes \theta_T \; Q \; \theta_T^{-1}) \; \boldsymbol{\mathcal{Y}}^\intercal \Big(\Theta_M(x) \otimes \Theta_N(t)\Big), \tag{3.17}$$

where I_{M+1} is the $(M+1)$ identity matrix, $\boldsymbol{\mathcal{Y}}^\intercal$ is obtained from Eq. (3.16) and $Q = \Big[q_{ij}\Big]$ for $0 \leq i, j \leq N$ denotes a diagonal $(N+1) \times (N+1)$ matrix, with its diagonal elements specified by $q_{ij} = \frac{1}{i+1}$.

Proof.: The left hand side of Eq. (3.17) can be expressed as

$$\int_0^t \Big(\Theta_M(x) \otimes \Theta_N(s)\Big) ds = \Theta_M(x) \otimes \int_0^t \Theta_N(s) \; ds. \tag{3.18}$$

By using Eq. (2.8), we have

$$\begin{aligned} \int_0^t \Theta_N(s) \; ds &= \int_0^t \theta_T \; \mathcal{B}_N(s) \; ds = \theta_T \int_0^t \mathcal{B}_N(s) \; ds = \theta_T \int_0^t \Big[1, s, s^2, ..., s^N\Big]^\intercal \; ds \\ &= \theta_T \Big[\int_0^t ds, \int_0^t s \; ds, \int_0^t s^2 \; ds, ..., \int_0^t s^N \; ds \Big]^\intercal \\ &= \theta_T \left[t, \frac{t^2}{2}, \frac{t^3}{3}, ..., \frac{t^{N+1}}{N+1} \right]^\intercal = t \; \theta_T \left[1, \frac{t}{2}, \frac{t^2}{3}, ..., \frac{t^N}{N+1} \right]^\intercal. \end{aligned} \tag{3.19}$$

The vector $\left[1, \frac{t}{2}, \frac{t^2}{3}, ..., \frac{t^N}{N+1}\right]^\intercal$ can be reformulated as follows

$$\left[1, \frac{t}{2}, \frac{t^2}{3}, ..., \frac{t^N}{N+1}\right]^\intercal = \begin{pmatrix} 1 & 0 & \dots & 0 \\ 0 & \frac{1}{2} & \dots & 0 \\ \vdots & \vdots & \ddots & \vdots \\ 0 & 0 & \dots & \frac{1}{N+1} \end{pmatrix} \Big[1, t, t^2, ..., t^N\Big]^\intercal = Q \; \mathcal{B}_N(t). \tag{3.20}$$

By using $\mathcal{B}_N(t) = \theta_T^{-1} \; \Theta_N(t)$ and substitute from Eq. (3.20) in Eq. (3.19), subsequently, Eq. (3.18) takes the form

$$\int_0^t \Big(\Theta_M(x) \otimes \Theta_N(s)\Big) ds = t \; \Big(\Theta_M(x) \otimes \theta_T \; Q \; \theta_T^{-1} \; \Theta_N(t)\Big), \tag{3.21}$$

by employing Eq. (2.7) in Eq. (3.21), we get

$$\int_0^t \Big(\Theta_M(x) \otimes \Theta_N(s)\Big) ds = t \; \Big(I_{M+1} \otimes \theta_T \; Q \; \theta_T^{-1}\Big)\Big(\Theta_M(x) \otimes \Theta_N(t)\Big), \tag{3.22}$$

As we stated before, by approximate the function $y(x,t) = t$ as $y_{MN}(x,t) \simeq \Big(\Theta_M(x) \otimes \Theta_N(t)\Big)^\intercal \; Y$, then Eq. (3.22) turns into

$$\int_0^t \Big(\Theta_M(x) \otimes \Theta_N(s)\Big) ds = \Big(I_{M+1} \otimes \theta_T \; Q \; \theta_T^{-1}\Big)\Big(\Theta_M(x) \otimes \Theta_N(t)\Big)\Big(\Theta_M(x) \otimes \Theta_N(t)\Big)^\intercal \; Y, \tag{3.23}$$

now, by substituting from Eq. (3.16) in Eq. (3.23), we get

$$\int_0^t \Big(\Theta_M(x) \otimes \Theta_N(s)\Big) ds = \Big(I_{M+1} \otimes \theta_T \; Q \; \theta_T^{-1}\Big) \; \boldsymbol{\mathcal{Y}}^\intercal \; \Big(\Theta_M(x) \otimes \Theta_N(t)\Big), \tag{3.24}$$

thus, the proof is completed. □

4. Implementation method of solution

In this section, we discuss how to apply a fully spectral tau technique for the ABC time fractional non-linear integro reaction-diffusion equations with spatiotemporal variable-order Eq. (1.1) and Eq. (1.2). Firstly, let us begin our method by approximation of the terms of (1.1) and the IBCs Eq. (1.2) in terms of the shifted Legendre space and time Kronecker produc.

By employing Eq. (2.4), Eq. (3.1) and Eq. (2.7), we can approximate ${}^{ABC}_{0}\mathcal{D}_{t}^{\xi(x,t)}\Phi(x,t)$ as follows

$$\begin{aligned} {}^{ABC}_{0}\mathcal{D}_{t}^{\xi(x,t)}\Phi(x,t) &= {}^{ABC}_{0}\mathcal{D}_{t}^{\xi(x,t)}\ \Psi^{\intercal}\left(\Theta_M(x)\otimes\Theta_N(t)\right) = \Psi^{\intercal}\left(\Theta_M(x)\otimes {}^{ABC}_{0}\mathcal{D}_{t}^{\xi(x,t)}\ \Theta_N(t)\right) \\ &= \Psi^{\intercal}\left(\Theta_M(x)\otimes \Upsilon^{\xi(x,t)}\ \Theta_N(t)\right) = \Psi^{\intercal}\left(I_{M+1}\otimes \Upsilon^{\xi(x,t)}\right)\left(\Theta_M(x)\otimes\Theta_N(t)\right). \end{aligned} \tag{4.1}$$

Also, we can approximate $\frac{\partial^2\Phi(x,t)}{\partial x^2}$ with the help of Eq. (2.4), Eq. (3.8) and Eq. (2.7) as follows

$$\begin{aligned} \frac{\partial^2\Phi(x,t)}{\partial x^2} &= \Psi^{\intercal}\left(\frac{\partial^2}{\partial x^2}\ \Theta_M(x)\otimes\Theta_N(t)\right) = \Psi^{\intercal}\left(D^{(2)}\ \Theta_M(x)\otimes\Theta_N(t)\right) \\ &= \Psi^{\intercal}\left(D^{(2)}\otimes I_{N+1}\right)\left(\Theta_M(x)\otimes\Theta_N(t)\right), \end{aligned} \tag{4.2}$$

where I_{N+1} is the $(N+1)$ identity matrix.

The nonlinear term $\Phi^2(x,t)$ can be approximated by utilizing Eq. (2.4) and Eq. (3.10) as follows

$$\Phi^2(x,t) = \Psi^{\intercal}\left(\Theta_M(x)\otimes\Theta_N(t)\right)\left(\Theta_M(x)\otimes\Theta_N(t)\right)^{\intercal}\Psi = \Psi^{\intercal}\ \Pi^{\intercal}\left(\Theta_M(x)\otimes\Theta_N(t)\right), \tag{4.3}$$

where $\left(\Theta_M(x)\otimes\Theta_N(t)\right)\left(\Theta_M(x)\otimes\Theta_N(t)\right)^{\intercal}\Psi = \Pi^{\intercal}\left(\Theta_M(x)\otimes\Theta_N(t)\right)$ and Π is computed like (3.11).

By knowing that the function $k(x,s)$ is approximated by using the shifted Legendre vectors as

$$k_{MN}(x,s) \simeq K^{\intercal}\left(\Theta_M(x)\otimes\Theta_N(s)\right), \tag{4.4}$$

where the elements of the matrix $K = \left[k_{ij}\right]_{i=0,j=0}^{M,N}$ are computed as in Eq. (2.5), then by using Eq. (2.4), Eq. (3.10) and Eq. (3.17), the following approximation is attained

$$\begin{aligned} \int_0^t k(x,s)\ \Phi(x,s)ds &= \int_0^t K^{\intercal}\left(\Theta_M(x)\otimes\Theta_N(s)\right)\left(\Theta_M(x)\otimes\Theta_N(s)\right)^{\intercal}\Psi\ ds \\ &= K^{\intercal}\ \Pi^{\intercal}\ \int_0^t\left(\Theta_M(x)\otimes\Theta_N(s)\right)ds \\ &= K^{\intercal}\ \Pi^{\intercal}\ (I_{M+1}\otimes\theta_T\ Q\ \theta_T^{-1})\ \mathcal{Y}^{\intercal}\left(\Theta_M(x)\otimes\Theta_N(t)\right). \end{aligned} \tag{4.5}$$

Now, by employing Eq. (2.4), Eq. (3.10) and Eq. (4.5), we can approximate $\left(\Phi(x,t)\right)^r\int_0^t k(x,s)\ \Phi(x,s)ds$ as follows

$$\begin{aligned}\Big(\Phi(x,t)\Big)^r \int_0^t k(x,s)\ \Phi(x,s)\ ds &= \Big(\int_0^t k(x,s)\ \Phi(x,s)\ ds\Big)\Big(\Theta_M(x)\otimes\Theta_N(t)\Big)^\intercal \Psi \\ &= K^\intercal\ \Pi^\intercal\ (I_{M+1}\otimes\theta_T\ Q\ \theta_T^{-1})\ \mathcal{Y}^\intercal\ \Big(\Theta_M(x)\otimes\Theta_N(t)\Big)\Big(\Theta_M(x)\otimes\Theta_N(t)\Big)^\intercal \Psi \\ &= K^\intercal\ \Pi^\intercal\ (I_{M+1}\otimes\theta_T\ Q\ \theta_T^{-1})\ \mathcal{Y}^\intercal\ \Pi^\intercal\ \Big(\Theta_M(x)\otimes\Theta_N(t)\Big),\end{aligned} \tag{4.6}$$

it must be noticed that, for $r=0$, the matrix $\mathcal{Y}^\intercal$ will be $(M+1)\times(N+1)$ identity matrix.

The source function $f(x,t)$ has the following shifted Legendre approximation

$$f(x,t) = F^\intercal\ \Big(\Theta_M(x)\otimes\Theta_N(t)\Big), \tag{4.7}$$

where $F=\Big[f_{ij}\Big]_{i=0,j=0}^{M,N}$ represents an $(M+1)\times(N+1)$ vector, where each entry can be computed analogously to that described in Eq. (2.5).

Finally, substituting Eqs. (2.4), (4.1), (4.2), (4.3), (4.6) and (4.7) into Eq. (1.1), we get

$$\begin{aligned}\Big(\Psi^\intercal\ \Big(I_{M+1}\otimes\Upsilon^{\xi(x,t)}\Big) - a_1\ \Psi^\intercal + a_2\ \Psi^\intercal\ \Pi^\intercal - a_3\ K^\intercal\ \Pi^\intercal\ \Big(I_{M+1}\otimes\theta_T\ Q\ \theta_T^{-1}\Big)\ \mathcal{Y}^\intercal\ \Pi^\intercal \\ - a_4\ \Psi^\intercal\ \Big(D^{(2)}\otimes I_{N+1}\Big) - F^\intercal\Big)\Big(\Theta_M(x)\otimes\Theta_N(t)\Big) = 0,\end{aligned} \tag{4.8}$$

The main objective is to determine the vector Ψ, which is currently unknown. To achieve this, we formulate a system of nonlinear algebraic equations with $(M-1)\times(N)$ of entries of Ψ by applying Eq. (2.3) for $\Big(\Theta_M(x)\otimes\Theta_N(t)\Big)$. Subsequently, we apply the tau method in the following manner

$$\begin{aligned}\Big(\Psi^\intercal\ \Big(I_{M+1}\otimes\Upsilon^{\xi(x,t)}\Big) - a_1\ \Psi^\intercal + a_2\ \Psi^\intercal\ \Pi^\intercal - a_3\ K^\intercal\ \Pi^\intercal\ \Big(I_{M+1}\otimes\theta_T\ Q\ \theta_T^{-1}\Big)\ \mathcal{Y}^\intercal\ \Pi^\intercal \\ - a_4\ \Psi^\intercal\ \Big(D^{(2)}\otimes I_{N+1}\Big) - F^\intercal\Big)\Big(J_l^{(M-1,M+1)}\otimes J_T^{(N,N+1)}\Big) = 0.\end{aligned} \tag{4.9}$$

Besides, the shifted Legendre approximations of the known functions $g(x), h_1(t)$ and $h_2(t)$ have the following forms

$$g(x) = G^\intercal\ \Big(\Theta_M(x)\otimes\Theta_N(0)\Big),\ h_1(t) = H_1^\intercal\ \Big(\Theta_M(0)\otimes\Theta_N(t)\Big),\ h_2(t) = H_2^\intercal\ \Big(\Theta_M(l)\otimes\Theta_N(t)\Big), \tag{4.10}$$

where $G=\Big[g_{ij}\Big]_{i=0,j=0}^{M,N}, H_1=\Big[h_{1ij}\Big]_{i=0,j=0}^{M,N}$ and $H_2=\Big[h_{2ij}\Big]_{i=0,j=0}^{M,N}$ represent $(M+1)\times(N+1)$ vectors, where each entry can be computed analogously to that described in Eq. (2.5).

Furthermore, based on Eq. (4.10), the IBCs satisfy an additional set of $(2N+M+1)$ algebraic equations, as outlined below

$$\begin{aligned}&\Big(\Psi^\intercal - G_1^\intercal\Big)\Big(J_l^{(M+1,M+1)}\otimes\Theta_N(0)\Big) = 0, \\ &\Big(\Psi^\intercal - H_1^\intercal\Big)\Big(\Theta_M(0)\otimes J_T^{(N,N+1)}\Big) = 0,\ \Big(\Psi^\intercal - H_2^\intercal\Big)\Big(\Theta_M(l)\otimes J_T^{(N,N+1)}\Big) = 0.\end{aligned} \tag{4.11}$$

Hereafter, we describe the implemented numerical simulation of the proposed model Eq. (1.1) and Eq. (1.2) using the following algorithm.

Algorithm

Input: $M, N, l, T, a_1, a_2, a_3, a_4, f(x,t), g(x), h_1(t), h_2(t), \xi(x,t)$
Step 1: produce the vectors $\Theta_N(t), \Theta_M(x)$ using Eq. (2.6).
Step 2: The unknown matrix Ψ is defined using Eq. (2.5), while the identity matrices I_{M+1} and I_{N+1}, as well as matrices $J_T^{(N,N+1)}$, $J_T^{(M-1,M+1)}$, and $J_L^{(M+1,M+1)}$, are defined according to Eq. (2.3), the matrices θT and θ_T^{-1} are specified by Eq. (2.9).
Step 3: Evaluate the matrices $\Upsilon^{\xi(x,t)}$ using (3.2), $\mathcal{T}_k$ using (3.3), $D^{(2)}$ using (3.9), $\mathcal{Y}$ using (3.16), Π using (4.3), K using (4.4), F using (4.7) and G, H_1, H_2 using (4.10).
Step 4: Combine the systems given in (4.9) and (4.11) and then solve for the matrix Ψ.
output: Following Eq. (2.4), we obtain $\Phi(x,t) \approx \Psi^\intercal \Big(\Theta_M(x) \otimes \Theta_N(t)\Big)$.

Remark 2: The proposed technique can be extended to solve Eq. (1.1) with variable coefficients (i.e. if $a_i \to a_i(x,t)$ for $i = 1,2,3,4$) , where the functions $a_i(x,t)$ can be approximated as follows

$$a_{iMN}(x,t) \simeq A_i^\intercal \Big(\Theta_M(x) \otimes \Theta_N(t)\Big) \simeq \Big(\Theta_M(x) \otimes \Theta_N(t)\Big)^\intercal A_i,\ i = 1,2,3,4, \tag{4.12}$$

then, by using Eqs. (2.4), (4.1), (4.2), (4.3), (4.6) (4.7), (4.12) and considering Eq. (1.1) with the variable coefficients, we get

$$\begin{aligned}
&\Psi^\intercal \Big(I_{M+1} \otimes \Upsilon^{\xi(x,t)}\Big)\Big(\Theta_M(x) \otimes \Theta_N(t)\Big) - \Psi^\intercal \Big(\Theta_M(x) \otimes \Theta_N(t)\Big)\Big(\Theta_M(x) \otimes \Theta_N(t)\Big)^\intercal A_1 \\
&+ \Psi^\intercal \Pi^\intercal \Big(\Theta_M(x) \otimes \Theta_N(t)\Big)\Big(\Theta_M(x) \otimes \Theta_N(t)\Big)^\intercal A_2 \\
&- K^\intercal \Pi^\intercal \Big(I_{M+1} \otimes \theta_T\, Q\, \theta_T^{-1}\Big)\, \mathcal{Y}^\intercal \Pi^\intercal \Big(\Theta_M(x) \otimes \Theta_N(t)\Big)\Big(\Theta_M(x) \otimes \Theta_N(t)\Big)^\intercal A_3 \\
&- \Psi^\intercal \Big(D^{(2)} \otimes I_{N+1}\Big)\Big(\Theta_M(x) \otimes \Theta_N(t)\Big)\Big(\Theta_M(x) \otimes \Theta_N(t)\Big)^\intercal A_4 - F^\intercal \Big(\Theta_M(x) \otimes \Theta_N(t)\Big) = 0,
\end{aligned} \tag{4.13}$$

by applying Eq. (3.10) in Eq. (4.13), we get

$$\begin{aligned}
\Big(\Psi^\intercal \Big(I_{M+1} \otimes \Upsilon^{\xi(x,t)}\Big) - \Psi^\intercal \mathcal{A}_1^\intercal + \Psi^\intercal \Pi^\intercal \mathcal{A}_2^\intercal - K^\intercal \Pi^\intercal \Big(I_{M+1} \otimes \theta_T\, Q\, \theta_T^{-1}\Big)\, \mathcal{Y}^\intercal \Pi^\intercal \mathcal{A}_3^\intercal \\
- \Psi^\intercal \Big(D^{(2)} \otimes I_{N+1}\Big)\mathcal{A}_4^\intercal - F^\intercal\Big)\Big(\Theta_M(x) \otimes \Theta_N(t)\Big) = 0,
\end{aligned} \tag{4.14}$$

where

$$\Big(\Theta_M(x) \otimes \Theta_N(t)\Big)\Big(\Theta_M(x) \otimes \Theta_N(t)\Big)^\intercal A_i = \mathcal{A}_i^\intercal \Big(\Theta_M(x) \otimes \Theta_N(t)\Big),\ i = 1,2,3,4. \tag{4.15}$$

Finally, a system of nonlinear algebraic equations with $(M-1) \times (N)$ of entries of Ψ by using the orthogonality relation Eq. (2.3).

5. Numerical examples

We illustrate the method's efficacy in this section by examining five particular examples. All calculations were performed with Mathematica 12.2 on a desktop computer featuring a 8 GB of RAM and Core™ i3-6100 CPU. The definitions for absolute error (AE), maximum absolute error

(MAE), and convergence order are provided as follows:

$$\text{AE} = \left|\Phi(x_i,t_j) - \Phi_{MN}(x_i,t_j)\right|,\ \text{MAE} = \max_{(x,t)\in[0,l]\times[0,T]} \left|\Phi(x,t) - \Phi_{MN}(x,t)\right|,$$

$$\text{CO} = \frac{\log(\text{MAE}(N_1)/\text{MAE}(N_2))}{\log(N_2/N_1)}.$$

Example 5.1. *Consider the NFIRDE with SVO, as given in Eq. (1.1). Set* $a_1 = a_2 = a_3 = a_4 = 1$, $r = 1$, $k(x,s) = xs$, *and* $\xi(x,t) = 1 - 0.3e^{-xt}$. *The IBCs and* $f(x,t)$ *match the exact solution* $\Phi(x,t) = e^{x-t}$.

The practical application of the proposed method is demonstrated on example by using different numbers of basis functions. The AEs, MAEs and COs at various values of M are presented in Table 1. Additionally, in the case of $M = N = 8$, we have depicted the resulting behaviour of the AE function and the corresponding contour error distribution in Figure 1.

TABLE 1. The AEs , MAEs and COs at $M = N$ for Example 5.1.

$x = t$	$M = 2$	$M = 3$	$M = 4$	$M = 5$	$M = 6$	$M = 7$	$M = 8$
0.2	7.70×10^{-3}	1.53×10^{-3}	1.20×10^{-4}	1.20×10^{-4}	1.21×10^{-8}	1.11×10^{-9}	4.25×10^{-11}
0.4	1.05×10^{-2}	3.03×10^{-3}	3.91×10^{-5}	3.91×10^{-5}	9.14×10^{-8}	1.80×10^{-9}	7.40×10^{-11}
0.6	6.56×10^{-3}	1.30×10^{-3}	6.72×10^{-6}	6.72×10^{-6}	5.77×10^{-8}	3.52×10^{-10}	5.71×10^{-11}
0.8	1.11×10^{-3}	4.46×10^{-4}	7.30×10^{-5}	1.19×10^{-4}	3.14×10^{-8}	7.24×10^{-10}	1.38×10^{-11}
MAEs	2.035×10^{-2}	4.383×10^{-3}	1.483×10^{-4}	1.471×10^{-4}	1.992×10^{-7}	5.174×10^{-9}	8.915×10^{-10}
COs	–	3.787	11.771	0.036	36.225	23.682	13.169

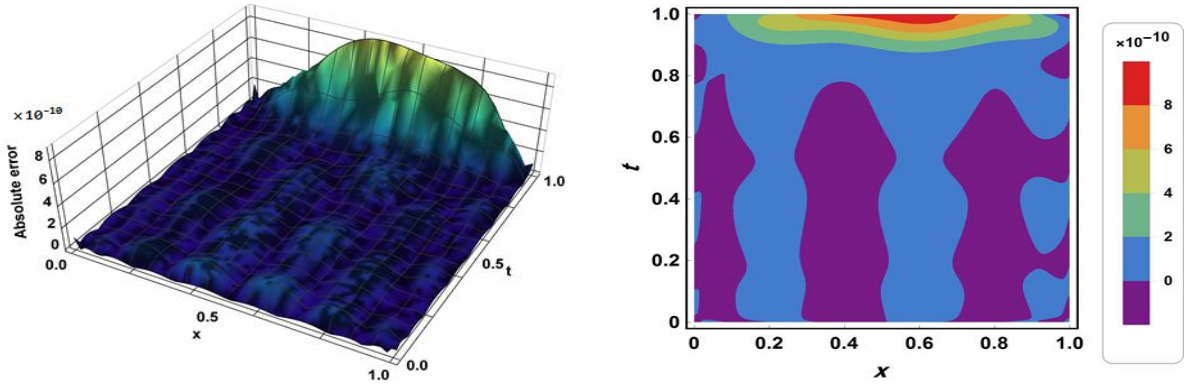

FIGURE 1. The behaviour of the AE function and the associated contour error distribution with $M = N = 8$ for Example 5.1.

Example 5.2. *Consider Eq. (1.1) with* a_3=a_4=1 *and* $k(x,s)$=1, *where the IBCs (1.2) and the source function* $f(x,t)$ *are agree with the exact solution* $\Phi(x,t) = \frac{(1-x^2)cosh(t)}{sinh^2(t)+2}$. *This example is considered with two cases:*
Case 1*:* a_1=a_2=1, r=1 *and three different spatiotemporal variable-order* $\xi(x,t)$.
Case 2*:* a_1=a_2=r=0 *and constant fractional order* $\xi(x,t)$=0.5 *[21, 36].*

TABLE 2. The AEs, MAEs and COs of Case 1 with different $\xi(x,t)$ with $M = 2$ for Example 5.2

$x = t$	$\xi(x,t) = 0.2 + 0.5\, e^{-x}\, sin(t)$			$\xi(x,t) = 1 - 0.3\, e^{xt}$			$\xi(x,t) = 0.25 + 0.6\ \lvert x - t\rvert$		
	$N = 4$	$N = 6$	$N = 8$	$N = 4$	$N = 6$	$N = 8$	$N = 4$	$N = 6$	$N = 8$
0.1	2.71×10^{-5}	4.85×10^{-7}	9.01×10^{-9}	2.69×10^{-5}	4.85×10^{-7}	9.00×10^{-9}	2.69×10^{-5}	4.90×10^{-7}	9.66×10^{-9}
0.3	5.75×10^{-5}	9.69×10^{-7}	1.42×10^{-9}	5.71×10^{-5}	9.69×10^{-6}	1.44×10^{-9}	5.76×10^{-5}	9.82×10^{-7}	5.72×10^{-10}
0.5	4.52×10^{-5}	8.22×10^{-7}	9.67×10^{-9}	4.58×10^{-5}	8.33×10^{-6}	9.72×10^{-9}	4.63×10^{-5}	8.23×10^{-7}	9.22×10^{-9}
0.7	1.43×10^{-5}	4.94×10^{-7}	1.41×10^{-8}	1.35×10^{-5}	5.14×10^{-6}	1.42×10^{-8}	1.52×10^{-5}	4.71×10^{-7}	1.41×10^{-8}
0.9	1.96×10^{-5}	4.46×10^{-7}	2.91×10^{-10}	1.97×10^{-5}	4.58×10^{-6}	5.58×10^{-10}	2.05×10^{-5}	4.22×10^{-7}	6.43×10^{-10}
MAEs	3.208×10^{-4}	$3,112 \times 10^{-6}$	3.787×10^{-8}	3.208×10^{-4}	$3,112 \times 10^{-6}$	3.787×10^{-8}	3.208×10^{-4}	7.608×10^{-6}	3.737×10^{-8}
COs	–	11.433	15.325	–	11.433	15.325	–	9.228	18.479

TABLE 3. Comparison the AEs of our method with other methods for Case 2 of Example 5.2

The proposed method		The method in [21]		The method in [36]		
x	AEs	x	AEs at Δt=0.00001	$\mathcal{M}$	AEs at Δt=0.0001	AEs at Δt=0.000001
0.2	1.16×10^{-8}	0.2	1.5×10^{-3}	10	9.4×10^{-4}	3.4×10^{-5}
0.4	1.52×10^{-8}	0.4	4.2×10^{-3}	15	7.1×10^{-4}	2.4×10^{-5}
0.6	1.14×10^{-8}	0.6	6.8×10^{-3}	20	4.6×10^{-4}	1.9×10^{-5}
0.8	9.95×10^{-10}	0.8	9.6×10^{-3}	30	4.0×10^{-4}	1.3×10^{-5}

We have practically applied the proposed method for this example with two different cases. In Case 1, the SVO NFIRDE is presented, while Case 2 deals with constant order linear fractional integro reaction-diffusion equation. The AEs, MAEs and COs with $M = 2$ and different values of N and spatiotemporal variable-order functions $\xi(x,t)$ for Case 1 are summarized in Table 2. It's clear that our method is highly precise for all different selected variable-order functions, even with a small number of bases functions. In Table 3, we compare the AEs generated by the proposed technique at $M = 2$, $N = 8$ at various values of $x = t$ with the AEs obtained from the quasi-wavelets based difference method in [21] for different x values and at time length $\Delta t = 0.00001$ and the AEs of the quasi-wavelets based Crank–Nicolson scheme in [36] at different number of nodes $\mathcal{M}$ at time lengths $\Delta t = 0.0001, 0.000001$. Regarding Table 3, the proposed method consistently yields highly accurate approximate solutions when compared with the methods in [21] and [36].

Example 5.3. *Consider the NFIRDE involving SVO in both space and time Eq. (1.1) with* a_1=a_2=a_3=a_4=1, $r = 1, k(x,s) = s\, e^{-x}$ *and* $\xi(x,t) = 0.8 + 0.005\, cos(xt)\, sin(x)$. *The IBCs and* $f(x,t)$ *match the exact solution* $\Phi(x,t) = x^2\,(1-x)^2\,(t^\beta + 1)$.

The proposed technique was tested in Example 5.3 with two different exact solutions: a smooth one with β = 4 and a nonsmooth one with β = 3.7. In the presence of a smooth exact solution, we have depicted the resulting behaviour of the AE function and the corresponding contour error distribution at M=N=5 in Figure 2. Additionally, in the case of a nonsmooth exact solution,

we have depicted the resulting behaviour of the AE function and the corresponding contour error distribution at M=4 and N=8 in Figure 3. As we know, spectral methods can be used on mathematical models with smooth solutions that preserve the property of spectral accuracy of the numerical solutions, which appears clearly from Figure 2, which gives accurate solutions using a few number of bases functions. However, in the case of non-smooth solutions, the spectral methods cause a deterioration in numerical results, and in order to overcome this, we have used an approximation using Legendre polynomials to preserve the stability and convergence of the numerical results and obtain accurate solutions. As a result, by using this approximation for the case of non-smooth solutions in Example 5.3, we obtain accurate numerical results as shown in Figure 3.

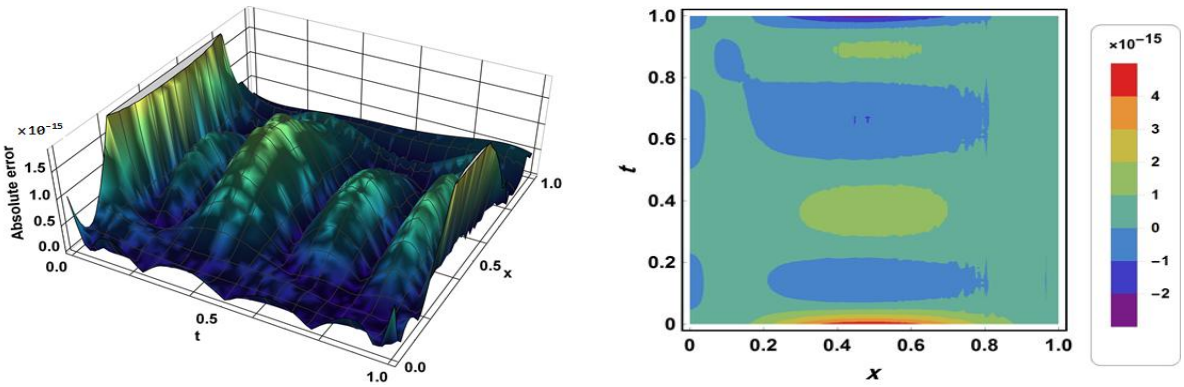

FIGURE 2. The behaviour of the AE function and the associated contour error distribution with β=4 and M=N=5 for Example 5.3.

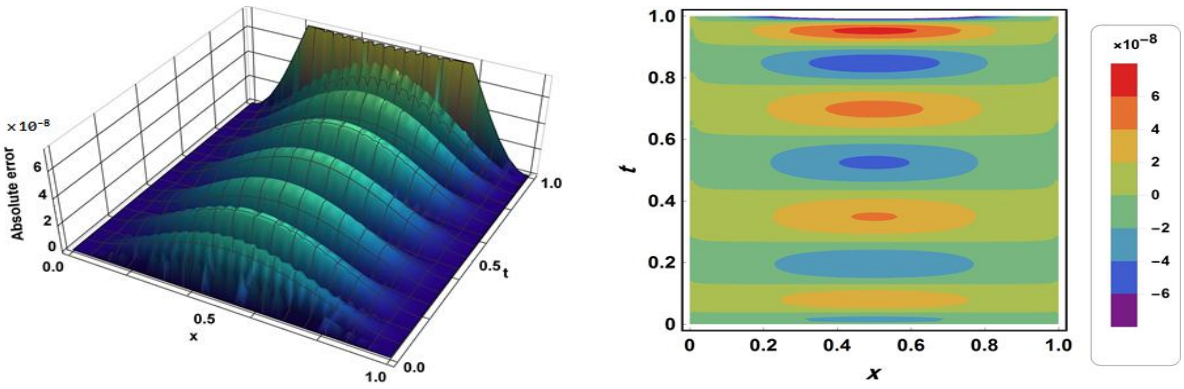

FIGURE 3. The behaviour of the AE function and the associated contour error distribution with β=3.7 and M=4, N=8 for Example 5.3.

Example 5.4. *Consider Eq. (1.1) with* a_1=a_2=a_4=1, r=1, $k(x,s)$=e^{-xs} *and* $\xi(x,t) = 1 - 0.7\,cos(xt)$. *The IBCs (1.2) and the source function* $f(x,t)$ *are agree with the exact solution* $\Phi(x,t) = (1+x^2)\,sin(t)$.

TABLE 4. The AEs, MAEs and COs at different values of N with $M = 2$ for Example 5.4

$x = t$	$a_3 = 1$				$a_3 = 0$			
	$N = 2$	$N = 4$	$N = 6$	$N = 8$	$N = 2$	$N = 4$	$N = 6$	$N = 8$
0.1	3.021×10^{-3}	5.257×10^{-6}	8.057×10^{-9}	1.097×10^{-11}	3.029×10^{-3}	5.303×10^{-6}	8.064×10^{-9}	1.098×10^{-11}
0.3	1.740×10^{-3}	1.302×10^{-5}	1.723×10^{-8}	3.188×10^{-11}	1.777×10^{-3}	1.313×10^{-5}	1.725×10^{-8}	3.167×10^{-12}
0.5	4.476×10^{-3}	1.308×10^{-5}	1.872×10^{-8}	1.571×10^{-11}	4.446×10^{-3}	1.293×10^{-5}	1.863×10^{-8}	1.568×10^{-11}
0.7	7.651×10^{-3}	7.487×10^{-6}	1.934×10^{-8}	3.251×10^{-11}	7.666×10^{-3}	7.675×10^{-6}	1.917×10^{-8}	3.248×10^{-11}
0.9	7.091×10^{-3}	3.255×10^{-5}	5.676×10^{-8}	1.537×10^{-11}	7.054×10^{-3}	3.253×10^{-5}	1.665×10^{-8}	1.541×10^{-11}
MAEs	2.867×10^{-2}	4.538×10^{-5}	2.011×10^{-7}	7.763×10^{-11}	2.867×10^{-2}	5.732×10^{-5}	8.019×10^{-8}	7.762×10^{-11}
COs	–	9.303	13.365	27.320	–	8.971	16.209	24.125

This example is considered with a_3=1 and a_3=0 which makes Eq. (1.1) represents the NFIRDE and reaction-diffusion equation with SVO, respectively. The AEs, MAEs and COs of both values of a_3 with M=2 and different values of N are tabulated in Table 4. Based on the obtained results in Table 4, it is evident that the obtained results satisfy consistently highly accurate solutions. Furthermore, the numerical solutions satisfy exponential improvement.

Example 5.5. *Consider Eq. (1.1) with* a_1=a_3=0, a_2=$sin(xt)$, a_4=$\frac{3}{2}$ *and* $\xi(x,t) = 0.65 + 0.2\ sin(xt)$. *The IBCs and* $f(x,t)$ *match the exact solution* $\Phi(x,t) = e^{-t}\ cos(x)$. *This equation represents the fractional reaction-diffusion involving SVO with variable coefficients.*

In this example, the proposed technique is applied to address the SVO nonlinear fractional reaction-diffusion equations with variable coefficients. Therefore, we apply Eq. (4.14) to obtain the approximate solution of this example. To assess the accuracy of the obtained approximate solutions, we compare the AEs generated by our method when $M = N$ with the AEs from the method in [35] at corresponding space-time points. As indicated in Table 5, our obtained approximate solutions exhibit slightly superior accuracy compared to the shifted second kind Chebyshev cardinal functions based method in [35]. Also, The behaviour of the AE function and the associated contour error distribution with $M = N = 8$ is plotted in Figure 4.

TABLE 5. The AEs at different values of the points $x = t$ and M with $N = 8$ for Example 5.5

x	The proposed method			The method in [35]		
	$M = 4$	$M = 6$	$M = 8$	$M = 4$	$M = 6$	$M = 8$
0.2	1.6623×10^{-5}	5.6441×10^{-9}	2.7156×10^{-11}	1.0655×10^{-4}	2.1943×10^{-7}	2.0632×10^{-10}
0.4	1.7099×10^{-5}	2.8430×10^{-8}	3.3150×10^{-11}	5.6745×10^{-5}	1.2581×10^{-7}	1.5469×10^{-10}
0.6	1.1975×10^{-5}	2.2521×10^{-8}	2.8068×10^{-11}	2.9110×10^{-5}	7.2059×10^{-7}	8.2828×10^{-11}
0.8	7.4003×10^{-6}	2.6617×10^{-9}	2.1131×10^{-12}	1.5575×10^{-5}	2.8359×10^{-8}	2.8559×10^{-11}

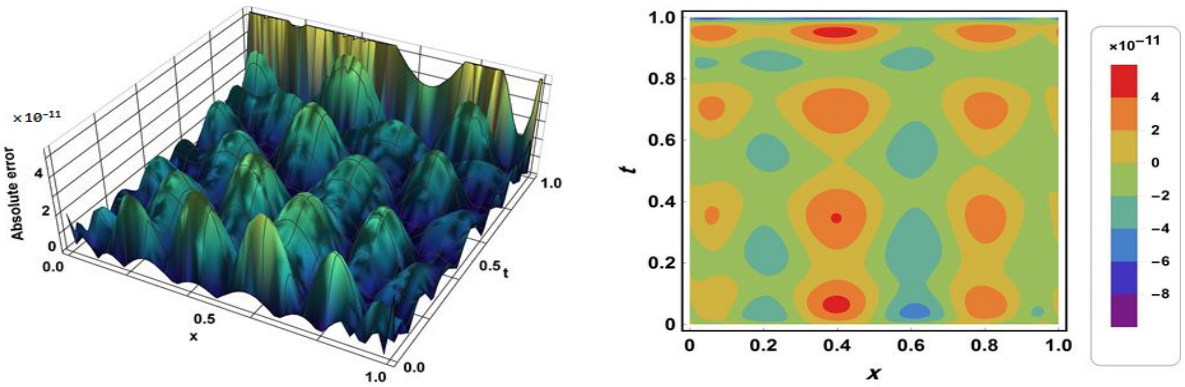

FIGURE 4. The behaviour of the AE function and the associated contour error distribution with $M = N = 8$ for Example 5.5.

6. Conclusion

In this paper a new nonlinear ABC NFIRDE with SVO has been presented. The main contributions of the presented work lied in deriving novel operational matrices for both SVO ABC fractional derivatives and integration. Based on these operational matrices and the operational matrix of the vector multiplications with the space-time Kronecker product, we presented a fully spectral tau technique that yielded a nonlinear algebraic system of equations without using any specific nodes. The authors believe that there is no previous work comprehensively utilizes the spectral tau technique for approximating solutions to the nonlinear integro-partial differential equations with ABC SVO time fractional derivative, this is the first instance of employing the fully spectral tau technique to solve constant or variable order nonlinear ABC fractional integro partial differential equations. The proposed method illustrated high accuracy and rapied convergence rate with both smooth and non-smooth solutions due to their non-local properties. Additionally, this method is well-suited for application to fractional nonlinear integro-differential equations with variable orders and higher dimensions.

Data Availability: Data sharing not applicable to this article as no datasets were generated or analyzed during the current study.

Acknowledgments: This project was funded by the Deanship of Scientific Reaserch (DSR) at King Abdulaziz University, Jeddah, under grant no. (GPIP:678-130-2024). The authors therfore, acknowledge with thanks DSR for technical and financial support.

Conflicts of Interest: The authors declare that there are no conflicts of interest regarding the publication of this paper.

References

[1] I. Podlubny, Fractional Differential Equations: An Introduction to Fractional Derivatives, Fractional Differential Equations, to Methods of Their Solution and Some of Their Applications, Academic Press, San Diego, 1998.

[2] H.F. Ahmed, W.A. Hashem, Novel and Accurate Gegenbauer Spectral Tau Algorithms for Distributed Order Nonlinear Time-Fractional Telegraph Models in Multi-Dimensions, Commun. Nonlinear Sci. Numer. Simul. 118 (2023), 107062. https://doi.org/10.1016/j.cnsns.2022.107062.

[3] L. Li, Z. Chen, H. Du, W. Jiang, B. Zhang, A Meshless Approach Based on Fractional Interpolation Theory and Improved Neural Network Bases for Solving Non-Smooth Solution of 2D Fractional Reaction–Diffusion Equation with Distributed Order, Commun. Nonlinear Sci. Numer. Simul. 138 (2024), 108245. https://doi.org/10.1016/j.cnsns.2024.108245.

[4] MM. Izadi, D. Baleanu, An Effective QLM-Based Legendre Matrix Algorithm to Solve the Coupled System of Fractional-Order Lane-Emden Equations, Appl. Numer. Math. 201 (2024), 608–627. https://doi.org/10.1016/j.apnum.2023.12.004.

[5] W. Hundsdorfer, J. Verwer, Numerical Solution of Time-Dependent Advection-Diffusion-Reaction Equations, Springer, Berlin, 2003. https://doi.org/10.1007/978-3-662-09017-6.

[6] F. Liu, V. Anh, I. Turner, Numerical Solution of the Space Fractional Fokker–Planck Equation, J. Comp. Appl. Math. 166 (2004), 209–219. https://doi.org/10.1016/j.cam.2003.09.028.

[7] Y. Kuramoto, Chemical Oscillations, Waves and Turbulence, Dover Publications, New York, 2003.

[8] T. Zhao, L. Zhao, Jacobian Spectral Collocation Method for Spatio-Temporal Coupled Fokker-Planck Equation with Variable-Order Fractional Derivative, Commun. Nonlinear Sci. Numer. Simul. 124 (2023), 107305. https://doi.org/10.1016/j.cnsns.2023.107305.

[9] J. Liu, X. Li, X. Hu, A RBF-Based Differential Quadrature Method for Solving Two-Dimensional Variable-Order Time Fractional Advection-Diffusion Equation, J. Comp. Phys. 384 (2019), 222–238. https://doi.org/10.1016/j.jcp.2018.12.043.

[10] M.H. Heydari, Z. Avazzadeh, Chebyshev–Gauss–Lobatto Collocation Method for Variable-Order Time Fractional Generalized Hirota–Satsuma Coupled KdV System, Eng. Comp. 38 (2022), 1835–1844. https://doi.org/10.1007/s00366-020-01125-5.

[11] H.G. Sun, W. Chen, H. Wei, Y.Q. Chen, A Comparative Study of Constant-Order and Variable-Order Fractional Models in Characterizing Memory Property of Systems, Eur. Phys. J. Spec. Topics 193 (2011), 185–192. https://doi.org/10.1140/epjst/e2011-01390-6.

[12] A. Habibirad, R. Roohi, E. Hesameddini, M.H. Heydari, A Reliable Algorithm to Determine the Pollution Transport within Underground Reservoirs: Implementation of an Efficient Collocation Meshless Method Based on the Moving Kriging Interpolation, Eng. Comp. 38 (2022), 2781–2795. https://doi.org/10.1007/s00366-021-01430-7.

[13] L.E.S. Ramirez, C.F.M. Coimbra, On the Variable Order Dynamics of the Nonlinear Wake Caused by a Sedimenting Particle, Physica D: Nonlinear Phen. 240 (2011), 1111–1118. https://doi.org/10.1016/j.physd.2011.04.001.

[14] N. Jacob, H.G. Leopold, Pseudo Differential Operators with Variable Order of Differentiation Generating Feller Semigroups, Integr. Equ. Oper. Theory 17 (1993), 544–553. https://doi.org/10.1007/BF01200393.

[15] O.T. Kolebaje, O.R. Vincent, U.E. Vincent, P.V.E. McClintock, Nonlinear Growth and Mathematical Modelling of COVID-19 in Some African Countries with the Atangana–Baleanu Fractional Derivative, Commun. Nonlinear Sci. Numer. Simul. 105 (2022), 106076. https://doi.org/10.1016/j.cnsns.2021.106076.

[16] C. Li, J. Liu, T. He, Fractional-Order Rate-Dependent Thermoelastic Diffusion Theory Based on New Definitions of Fractional Derivatives with Non-Singular Kernels and the Associated Structural Transient Dynamic Responses Analysis of Sandwich-like Composite Laminates, Commun. Nonlinear Sci. Numer. Simul. 132 (2024), 107896. https://doi.org/10.1016/j.cnsns.2024.107896.

[17] A. Atangana, D. Baleanu, New Fractional Derivatives with Nonlocal and Non-Singular Kernel: Theory and Application to Heat Transfer Model, arXiv:1602.03408 [math.GM] (2016). http://arxiv.org/abs/1602.03408

[18] A. Atangana, J.F. Gómez-Aguilar, Fractional Derivatives with No-Index Law Property: Application to Chaos and Statistics, Chaos Solitons Fractals 114 (2018), 516–535. https://doi.org/10.1016/j.chaos.2018.07.033.

[19] J. Hristov, On the Atangana–Baleanu Derivative and Its Relation to the Fading Memory Concept: The Diffusion Equation Formulation, in: J.F. Gómez, L. Torres, R.F. Escobar (Eds.), Fractional Derivatives with Mittag-Leffler Kernel, Springer, Cham, 2019: pp. 175–193. https://doi.org/10.1007/978-3-030-11662-0_11.

[20] U. Ali, H. Ahmad, J. Baili, T. Botmart, M.A. Aldahlan, Exact Analytical Wave Solutions for Space-Time Variable-Order Fractional Modified Equal Width Equation, Results Phys. 33 (2022), 105216. https://doi.org/10.1016/j.rinp.2022.105216.

[21] S. Kumar, P. Pandey, Quasi Wavelet Numerical Approach of Non-Linear Reaction Diffusion and Integro Reaction-Diffusion Equation with Atangana–Baleanu Time Fractional Derivative, Chaos Solitons Fractals 130 (2020), 109456. https://doi.org/10.1016/j.chaos.2019.109456.

[22] S. Kondo, How Animals Get Their Skin Patterns: Fish Pigment Pattern as a Live Turing Wave, in: S. Nakanishi, R. Kageyama, D. Watanabe (Eds.), Systems Biology, Springer Japan, Tokyo, 2009: pp. 37–46. https://doi.org/10.1007/978-4-431-87704-2_4.

[23] H. Wilhelmsson, E. Lazzaro, Reaction-Diffusion Problems in the Physics of Hot Plasmas, CRC Press, 2000.

[24] J.D. Murray, ed., Mathematical Biology: II: Spatial Models and Biomedical Applications, Springer, New York, 2003. https://doi.org/10.1007/b98869.

[25] S. Guo, L. Mei, Y. Li, An Efficient Galerkin Spectral Method for Two-Dimensional Fractional Nonlinear Reaction–Diffusion-Wave Equation, Comp. Math. Appl. 74 (2017), 2449–2465. https://doi.org/10.1016/j.camwa.2017.07.022.

[26] A.S. Hendy, L. Qiao, A. Aldraiweesh, M.A. Zaky, Optimal Spectral Galerkin Approximation for Time and Space Fractional Reaction-Diffusion Equations, Appl. Numer. Math. 201 (2024), 118–128. https://doi.org/10.1016/j.apnum.2024.02.013.

[27] S. Maji, S. Natesan, Analytical and Numerical Solutions of Time-Fractional Advection-Diffusion-Reaction Equation, Appl. Numer. Math. 185 (2023), 549–570. https://doi.org/10.1016/j.apnum.2022.12.013.

[28] M. Hajipour, A. Jajarmi, D. Baleanu, H. Sun, On an Accurate Discretization of a Variable-Order Fractional Reaction-Diffusion Equation, Commun. Nonlinear Sci. Numer. Simul. 69 (2019), 119–133. https://doi.org/10.1016/j.cnsns.2018.09.004.

[29] S. Kumar, P. Pandey, Quasi Wavelet Numerical Approach of Non-Linear Reaction Diffusion and Integro Reaction-Diffusion Equation with Atangana–Baleanu Time Fractional Derivative, Chaos Solitons Fractals 130 (2020), 109456. https://doi.org/10.1016/j.chaos.2019.109456.

[30] H.-D. Qu, X. Liu, X. Lu, M. Ur Rahman, Z.-H. She, Neural Network Method for Solving Nonlinear Fractional Advection-Diffusion Equation with Spatiotemporal Variable-Order, Chaos Solitons Fractals 156 (2022), 111856. https://doi.org/10.1016/j.chaos.2022.111856.

[31] S. Kumar, Crank-Nicolson Quasi-Wavelet Method for the Numerical Solution of Variable-Order Time-Space Riesz Fractional Reaction-Diffusion Equation, in: Applications of Fractional Calculus to Modeling in Dynamics and Chaos, Chapman and Hall/CRC, pp. 407–428, 2022.

[32] H.F. Ahmed, W.A. Hashem, A Fully Spectral Tau Method for a Class of Linear and Nonlinear Variable-Order Time-Fractional Partial Differential Equations in Multi-Dimensions, Math. Comp. Simul. 214 (2023), 388–408. https://doi.org/10.1016/j.matcom.2023.07.023.

[33] H.F. Ahmed, M.B. Melad, A New Numerical Strategy for Solving Nonlinear Singular Emden-Fowler Delay Differential Models with Variable Order, Math. Sci. 17 (2023), 399–413. https://doi.org/10.1007/s40096-022-00459-z.

[34] F. Asadi-Mehregan, P. Assari, M. Dehghan, Numerical Simulation of Spatio-Temporal Spread of an Infectious Disease Utilizing a Collocation Method Based on Local Radial Basis Functions, Eng. Comp. 40 (2024), 2473–2496. https://doi.org/10.1007/s00366-023-01924-6.

[35] M.H. Heydari, A. Atangana, Z. Avazzadeh, M.R. Mahmoudi, An Operational Matrix Method for Nonlinear Variable-Order Time Fractional Reaction–Diffusion Equation Involving Mittag-Leffler Kernel, Eur. Phys. J. Plus 135 (2020), 237. https://doi.org/10.1140/epjp/s13360-020-00158-5.

[36] S. Kumar, J. Cao, X. Li, A Numerical Method for Time-Fractional Reaction-Diffusion and Integro Reaction-Diffusion Equation Based on Quasi-Wavelet, Complexity 2020 (2020), 3291723. https://doi.org/10.1155/2020/3291723.

[37] M.Y. Hussaini, T.A. Zang, Spectral Methods in Fluid Dynamics, Ann. Rev. Fluid Mech. 19 (1987), 339–367. https://doi.org/10.1146/annurev.fl.19.010187.002011.

[38] M.A. Zaky, An improved tau method for the multi-dimensional fractional Rayleigh–Stokes problem for a heated generalized second grade fluid, Comp. Math. Appl. 75 (2018), 2243–2258. https://doi.org/10.1016/j.camwa.2017.12.004.